Bloodstain Classification in Forensic Analysis Using Optimized 3D CNN

Abstract—Blood stain detection is essential in crime scene analysis as it provides valuable insights into the events that transpired, aids in identifying individuals involved and supports the investigation process of criminal cases. It helps investigators understand what happened, who was involved and when it occurred. Advancements in forensic science, particularly bloodstain analysis, have become imperative for enhancing crime scene reconstruction. Conventional methods like DNA analysis,chemical analysis often takes more time to identify bloodstain. Instead of DNA analysis this research contributes to the advancement of forensic science by introducing an innovative approach to bloodstain identification and classification by using a 3D CNN model utilizing the capabilities of Hyperspectral Imaging. Here we introduce an optimized 3D CNN with mish activation function and finding the best accuracy. This work will help to make faster investigations of forensic scene analysis and analyzing criminal cases.By applying the optimized 3D CNN model we get 97% accuracy which is higher than the existing 3D CNN (95%) and hybrid CNN(96%) model and parameters are reduced from 291895 to 125943.

Index Terms—Blood Strain Classification, Optimized 3D-CNN, Forensic Science,Crime scene analysis,Hyperspectral Image,mish,principal component analysis (PCA).

I. INTRODUCTION

In Dynamic criminal investigation, the field of forensic science plays a pivotal role in collecting, detecting, and analyzing evidence to facilitate successful case resolution.The examination of body fluids, particularly bloodstains holds significant importance during violent crime scenes as an integral aspect of forensic science [1]–[4]. The existences of blood at such scenes makes it a valuable forensic evidence, presenting challenges and opportunities for thorough analysis. Collecting, detecting and analyzing evidence from a crime scene is extremely challenging for a successful and active criminal investigation [5].

Body fluids are considered a crucial asset in forensic inquiries, especially in violent crime scenes. Among these, blood holds the highest importance in forensic analysis [6]. To identify bloodstain and the age of the bloodstains are crucial for solving a problem. By looking at how blood is spread out, we can understand what happened during the crime and maybe even identify who was involved in crime. Determining the age of bloodstains helps us piece together the timeline of events, which is important for finding suspects [7].

Our main target is to create a way to definitively verify that a stain is truly made up of blood. Visually bloodstains are similar with other substances ,in color and appearance. This similarity complicates the differentiation process. Identifying genuine bloodstains for DNA testing is crucial in forensic

investigations to avoid wasting time and resources on false positives, such as stains that may appear brown or similar to blood but are not actually blood. Dried bloodstains undergo various transformations as they age, resulting in alterations in color, texture. The identification of dried blood has emerged as an intriguing challenge in forensic science [8].

To estimate the depth of wound can be examined by the the spectral components of blood. The main key componete of blood is Hemoglobin derivatives, namely methemoglobin (metHB) and oxyhemoglobin (oxyHb). The distinctive spectral peaks of metHB and oxyHb in the VIS range spectra enable their identification and differentiation from other substances [9]. This is very important to understand how these entities behave when confronted with images that exhibit variations in both spatial and spectral features.

For our work,we use a publicly available HSI dataset that ensures transparency and accessibility [10]. Due to the HSI dataset's characteristics of having high spectral but low spatial information, conventional 1-D and 2-D Convolutional Neural Networks (CNNs) are not appropriate for this task. These networks would only handle spectral data, neglecting spatial information. To overcome this limitation, 3D CNN is more suitable. These models process data across three dimensions concurrently, allowing for the effective learning of hierarchical features. This approach need less parameters than 1D, 2D CNN and minimizing the information loss.

II. RELATED WORK

Hyperspectral imaging is a novel imaging technique gaining momentum in medical realms, especially for disease diagnosis and providing visual guidance during surgical procedures [11].

Hyperspectral imaging (HSI) is a method used in forensic science because it is quick, doesn't cause any damage, and doesn't require physical contact with the evidence [15].

Forensic labs employ different approaches to identify bloodstains. Presumptive tests are initial assessments that provide an indication but may not confirm definitively. The Kastle-Meyer (KM) test is specifically highlighted as one of the presumptive tests employed in forensic labs.The specificity of the KM reaction compared to benzidine in identifying stains from various sources such as bodily fluids, fruits, vegetables, and chemicals. The KM reaction exhibits higher specificity in contrast to benzidine [12].

Besides,Luminol is highly regarded and widely recognized as one of the most significant assays (tests or analyses) in forensic science.Luminol's effectiveness can be influenced by environmental conditions like ambient light, humidity, and

temperature can impact the sensitivity and reliability of the test. This work compares different luminol formulations that focus on their luminescence and longevity [13].

Advancements in laser technology and light detectors have significantly enhanced spectroscopic methods for characterizing molecules. These improvements have opened up new opportunities for on-site, conclusive identification of body fluids at crime scenario [14].

In the paper [12], they analyzed reflectance spectra from 35 stains that were not blood and 40 stains that were bloodstains, all of which were on white cotton fabric.

All the models that were tested demonstrated an ability to accurately identify deposited stains as blood, with a maximum accuracy of 94% and a minimum accuracy of 81% . The analysis resulted in correctly classifying 92% of the spectra during a leave-one-out cross-validation (LOOCV) process, where each spectrum was temporarily excluded from the model's training set and then tested against the model [15], [16].

The identification of blood traces is facilitated by non-contact techniques, primarily due to challenges in maintaining temperature and humidity with traditional methods.

Researchers turned to Hyperspectral Imaging (HSI) as it allows blood identification without contact that reduce the risk of destruction . The advantages include rapid data collection, no need for sample preparation and reduced workload in laboratories [17].

The current methods for detecting and identifying blood stains, involving visual examination and presumptive tests, have limitations such as false positives and potential interference with DNA tests. They introduced a new way of using hyperspectral imaging, specifically in the visible wavelength range, to detect and confirm blood stains on different colored surfaces without touching or damaging them. The method is capable of distinguishing between blood stains and nine other substances that are red in color, as well as identifying blood approximately from 40 reddish stains [18].

The paper [19] introduced an Active Learning (AL) pipeline aimed at addressing the challenge of sample selection in hyperspectral image (HSI) classification. They utilized deep convolution networks with a hybrid dilated residual approach, aiming to improve HSI classification performance by adaptively selecting spectral bands and overcoming limitations associated with manually crafted selections. In this paper [20], they improved the robustness of hyperspectral image classification by investigating the application of Deep Support Vector Machine (DSVM) with various kernel functions.

The challenge of stain detection is particularly in confirming whether in a crime scene a stain is a bloodstain or not. To overcome this difficulty, the confirmation of bloodstains is difficult, especially considering the implications of false positives.Deoxyribonucleic Acid (DNA) analysis is a powerful method for identifying suspects, but this approach is very expensive ,more costly and time consuming . Consequently, if a false positive occurs, such as with a stain that appears similar to blood but is not, it waste not only significant time but also

waste resources . SO,it is important to develop accurate and efficient methods for confirming bloodstains at crime scenes to avoid potential false positives and the associated costs and resources.

III. DATASET

Hyperspectral image contains both spatial and spectral information.For detection and classification of blood hyperspectral imaging has the ability to detect different forms of hemoglobin .
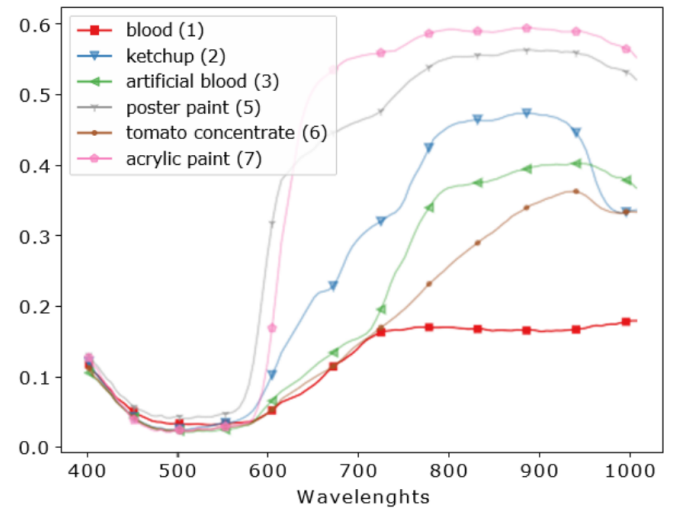

Fig. 1: Spectral signatures of experimental samples

The dataset contains different types of materials including blood, blood-like components, poster paint,ketchup, acrylic paint, beetroot juice,artificial blood,uncertain blood,tomato concentrate shown in Fig 2.
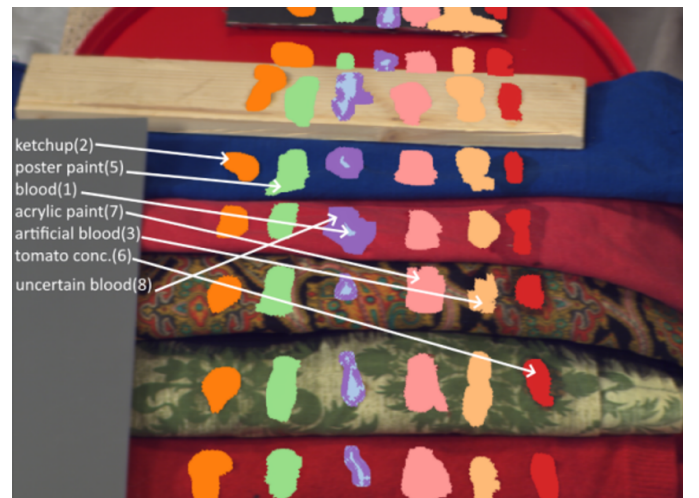

Fig. 2: Substances present in dataset

Over the span of three weeks, an array of images was captured, each possessing its unique ambiance crafted by

varying backgrounds and intensities of illuminating light. The images were captured over a three-week period and vary in terms of background composition and lighting intensity.

This dataset has 14 hyperspectral images which are in ENVI format. The images containing blood and similar substances like tomato concentrate , artificial blood , acrylic paint . Over the span of three weeks, an array of images was captured, each possessing its unique ambiance crafted by varying backgrounds and intensities of illuminating light. Each image size is 519×696 pixels (each pixel contains 113 band). Number of class is 7.

IV. METHODOLOGY

Hyperspectral image data is like a three-dimensional cube where each point represents a pixel in an image.It contains information about both the color and location of each pixel. This cube is made up of width, height and depth, where depth represents the number of different colors or spectral bands captured in the image. Each pixel is labeled with a vector indicating its category, with similarities and differences existing within each category. The image may contain overlapping categories, making it challenging to distinguish them accurately. To simplify this complex data, preprocessing is done using Principal Component Analysis (PCA) , reduced the number of colors while preserving important spatial information, thereby aiding in analysis and interpretation.

To effectively process hyperspectral imaging (HSI) data for image classification, a three-dimensional Convolutional Neural Network (3D CNN) is employed, utilizing its unique structure tailored for analyzing spatial-spectral information.

First of all, the HSI cube is divided into small overlapping 3D patches to analyze individual pixels closely. These patches enabling localized analysis centered around individual pixels. These patches are then fed into the 3D CNN, which comprises multiple layers of 3D convolutional operations. Unlike traditional 2D CNNs, which analyze spatial information only, the 3D CNN operates on both spatial and spectral dimensions simultaneously, enabling it to capture complex spatial-spectral patterns inherent in HSI data. The structure of the 3D CNN includes multiple layers of 3D convolutional kernels followed by activation functions to introduce nonlinearity.

In this image classification algorithms, the process begins by dissecting the HSI cube into smaller overlapping 3D-patches. These patches are meticulously crafted, with their truth labels discerned based on the central pixel's label. Following this initial step, neighbor patches $Np \in \mathbb{R}^{w \times w \times B}$ are crafted, employing a spatial window of $w \times w$ centered around specific spatial coordinates (x, y) . Each of these neighbor patches, denoted as n patches, covers a designated area, spanning the width and height dimensions of the HSI cube.

This coverage ranges from $(x - w + 1/2)$ to $(x + w - 1/2)$ and $(y - w + 1/2)$ to $(y + w - 1/2)$. In 3D CNN , 3D convolutional procedures and 3D kernel extracts spatial and spectral information from HSI cube.

Instead of the commonly used ReLU function, the Mish activation function is used here to enhance feature extraction

and learning capabilities. This function introduces smoothness and better gradients compared to ReLU, thereby improving the learning process. The 3D CNN architecture, augmented with the Mish activation function, effectively processes HSI data, extracting discriminative spatial-spectral features crucial for accurate image classification tasks.

The Mish activation function is defined as

$$f(x) = x \cdot \tanh(\ln(1 + e^x))$$

3×3 karnel size is used . Table-1 shows other details . The proposed model contains 125043 trainable parameters.Here "Adam" optimizer is used for optimizing the softmax function. For train and validate the 3D CNN model 10 epochs are used.

TABLE I: Proposed 3D CNN architecture model summary (Window size is 9×9)

Layer (type)	Output Shape	Param #
input_1 (InputLayer)	[(None, 9, 9, 15, 1)]	0
conv3d_1 (Conv3D)	(None, 7, 7, 9, 8)	512
conv3d_2 (Conv3D)	(None, 5, 5, 5, 16)	5776
conv3d_3 (Conv3D)	(None, 3, 3, 3, 32)	13856
conv3d_4 (Conv3D)	(None, 1, 1, 1, 64)	55360
flatten_1 (Flatten)	(None, 64)	0
dense_1 (Dense)	(None, 256)	16640
dense_2 (Dense)	(None, 128)	32896
dense_3 (Dense)	(None, 7)	903
Total params: 125943 (491.96 KB)		
Trainable params: 125943 (491.96 KB)		
Non-trainable params: 0 (0.00 Byte)		

V. EXPERIMENTAL SETUP

This data set is available online (www.kaggle.com) and experimented on an online platform Kaggle.com . Kaggle provides free access to NVIDIA TESLA P100 GPUs. Kaggle offers a generous allocation of cold storage, providing users with 358.27 GB of storage space. Additionally, Kaggle generously allocates a substantial amount of Random Access Memory (RAM), providing users with 25 GB of memory to efficiently handle large datasets and complex computational tasks.

This experiment is divided into three separate sets (Train/Validation/Test).These sets are Training (1690, 9, 9, 15, 1) Validation (1690, 9, 9, 15, 1) Test (30424, 9, 9, 15, 1) . The whole dataset is spilt into three ratio . Here Training : Validation : Test is 5% : 5% : 90% .For training purpose 5% is used and 5% is used for validation purpose and rest of the 90% is considered as test set .

VI. CLASSIFICATION RESULT

15 most informative band is selected by using the principle component analysis (PCA) method. While training the model 0.001 learning rate is used.

In comparison the proposed 3D CNN model's overall accuracy (OA) is higher than the traditional 3D CNN model. Before Optimizing the CNN model traditional ReLU activation function is used and after optimizing the 3D CNN model
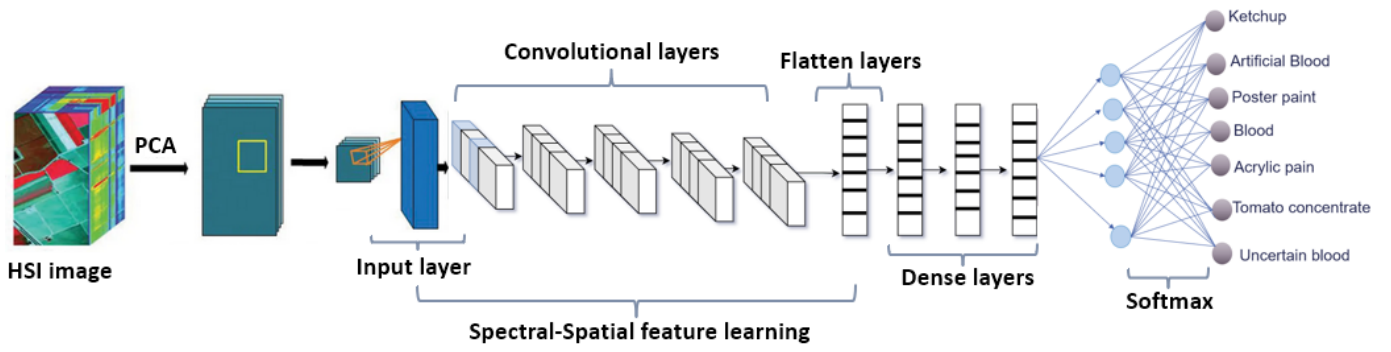
Fig. 3: Optimized 3D CNN (Kernel size =$3 \times 3 \times 7$, $3D_{input} = 9, 9, 15, 1$)
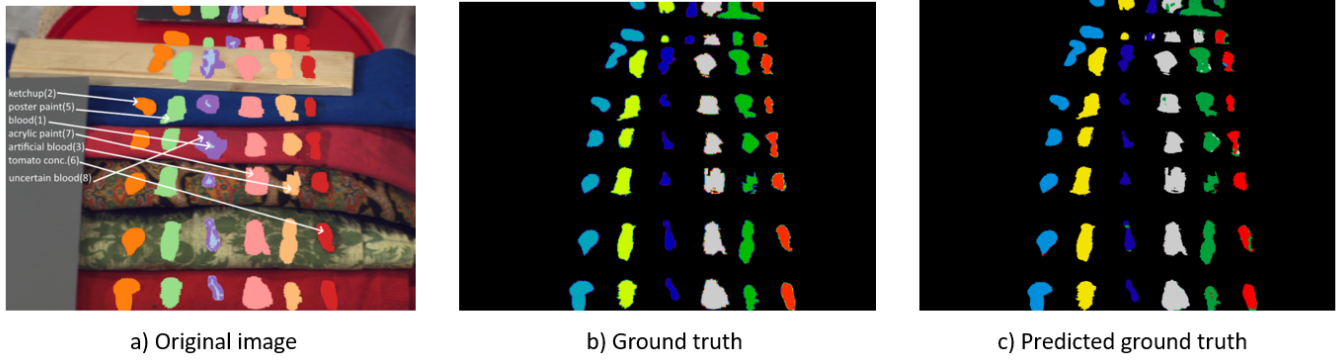

a) Original image   b) Ground truth   c) Predicted ground truth

Fig. 4: Original image, Ground truth and Predicted ground truth after 3D CNN

(a) Confusion matrix of 3D CNN [8] (b) Confusion matrix of Optimized 3D CNN

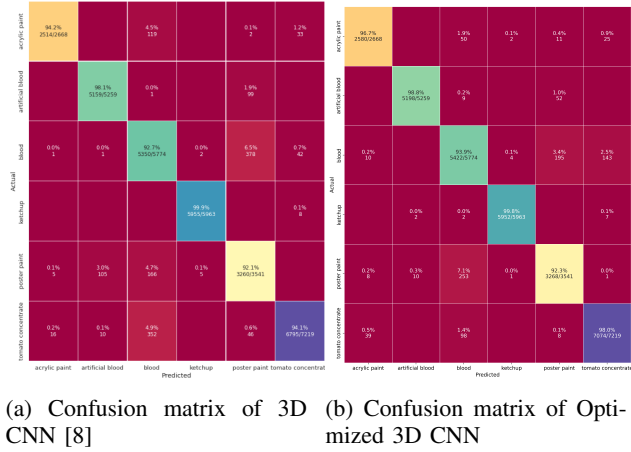Fig. 5: Confusion matrix curve

TABLE II: Classification Results using Optimized 3D CNN Model

Class	Precision	Recall	F1-Score	Support
blood	0.99	0.96	0.97	2668
ketchup	1.00	0.98	0.99	5259
artificial blood	0.93	0.92	0.93	5774
poster paint	1.00	1.00	1.00	5963
tomato concentrate	0.89	0.93	0.91	3541
acrylic paint	0.98	0.98	0.98	7219
Accuracy		0.97		
Macro Avg	0.96	0.96	0.96	30424
Weighted Avg	0.97	0.97	0.97	30424

Classifiers	Accuracy	Macro avg	Weighted avg	Parameter
3D CNN	0.95	0.95	0.95	291895
Hybrid CNN	0.96	0.97	0.96	291895
Optimized 3D CNN	0.97	0.96	0.97	125943

TABLE III: Classifier Performance

TABLE IV: Comparison of Precision, Recall, and F1-Score ("1" refer to 3D CNN and "2" refer to Optimized 3D CNN)

Class	Pre1	Pre2	Re1	Re2	F1-Sc1	F1-Sc2
blood	0.99	0.99	0.94	0.96	0.97	0.97
ketchup	0.98	1.00	0.98	0.98	0.98	0.99
artificial blood	0.89	0.93	0.93	0.92	0.91	0.93
poster paint	1.00	1.00	1.00	1.00	1.00	1.00
tomato concentrate	0.86	0.89	0.92	0.93	0.89	0.91
acrylic paint	0.99	0.98	0.94	0.98	0.96	0.98

we use mish activation function and in output layers softmax function is used. Whole evaluation result curves are shown in Table-II.

Here some comparison curve including confusion matrix, precision, recall and f1-score curve shown in Table-IV and figure 7 . The overall accuracy is increased from 95% to 97% .
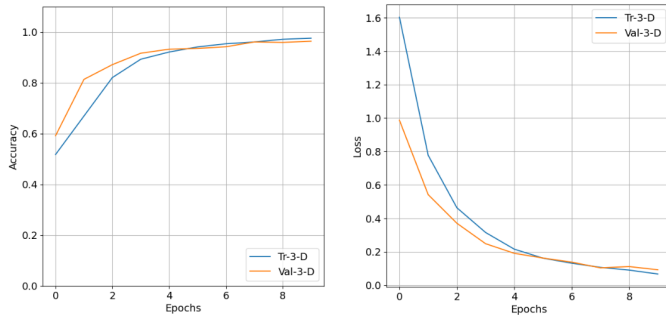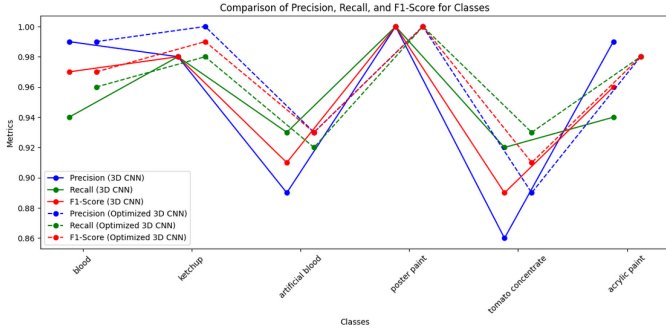
Fig. 6: Learning curve of Optimized 3D CNN

Fig. 7: Class wise Precision,Recall and F1-score Curve

VII. CONCLUSION

In this experiment we apply a 3D CNN architecture [8] and optimize this architecture with some changes in model layers and use mish activation function instead of relu function. The optimized model gives better accuracy than the existing one. By applying the optimized 3D CNN model we get 97% accuracy which is higher than the existing 3D CNN (95%) and hybrid CNN(96%) model and parameters are reduced from 291895 to 125943.
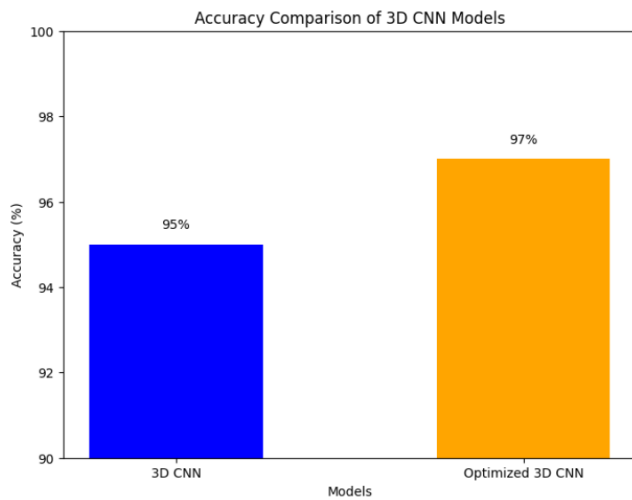

Fig. 8: Overall Accuracy Comparison

For this experiment the whole dataset is divided into three

separate sets. For training purpose 5% is used and 5% is used for validation purpose and rest of the 90% is considered as test set .In this experiment mish function works well as it is a non monotonic function, possess self-regularization properties, vanishing gradient problem which makes it better than relu activation functions.

VIII. FUTURE WORK

In this work we apply PCA for dimensionality reduction ignoring other technique.Though it is a good technique but there are some disadvatages . PCA is a unsupervised method . Our dataset contains available class information. As PCA is a unsupervised method it cannot utilize all information. Again it extract only linear informations.So for future study we will apply other non linear method like LDA, FDA, PLSR etc to get higher accuracy as our main focus is on increasing accuracy.

REFERENCES

[1] K. Ksiażek, M. Romaszewski, P. Głomb, B. Grabowski, and M. Cholewa, "Blood stain classification with hyperspectral imaging and deep neural networks," *Sensors*, vol. 20, no. 22, p. 6666, 2020.

[2] X. Liu, Q. Sun, B. Liu, B. Huang, and M. Fu, "Hyperspectral image classification based on convolutional neural network and dimension reduction," in *2017 Chinese automation congress (CAC)*, pp. 1686–1690, IEEE, 2017.

[3] E. De Vittori, F. Barni, S. W. Lewis, G. Antonini, C. Rapone, and A. Berti, "Forensic application of a rapid one-step tetramethylbenzidine-based test for the presumptive trace detection of bloodstains at the crime scene and in the laboratory," *Forensic Chemistry*, vol. 2, pp. 63–74, 2016.

[4] R. Rosenblatt, L. Halámková, K. C. Doty, E. A. de Oliveira Jr, and I. K. Lednev, "Raman spectroscopy for forensic bloodstain identification: method validation vs. environmental interferences," *Forensic Chemistry*, vol. 16, p. 100175, 2019.

[5] T. Wu, F. Breitinger, and S. O'Shaughnessy, "Digital forensic tools: Recent advances and enhancing the status quo," *Forensic Science International: Digital Investigation*, vol. 34, p. 300999, 2020.

[6] I. P. Hurley, R. Cook, C. W. Laughton, N. A. Pickles, H. E. Ireland, and J. H. Williams, "Detection of human blood by immunoassay for applications in forensic analysis," *Forensic science international*, vol. 190, no. 1-3, pp. 91–97, 2009.

[7] K. G. de Bruin, R. D. Stoel, and J. C. Limborgh, "Improving the point of origin determination in bloodstain pattern analysis," *Journal of forensic sciences*, vol. 56, no. 6, pp. 1476–1482, 2011.

[8] M. H. F. Butt, H. Ayaz, M. Ahmad, J. P. Li, and R. Kuleev, "A fast and compact hybrid cnn for hyperspectral imaging-based bloodstain classification," in *2022 IEEE Congress on Evolutionary Computation (CEC)*, pp. 1–8, IEEE, 2022.

[9] R. Gautam, D. Peoples, K. Jansen, M. O'Connor, G. Thomas, S. Vanga, I. J. Pence, and A. Mahadevan-Jansen, "Feature selection and rapid characterization of bloodstains on different substrates," *Applied spectroscopy*, vol. 74, no. 10, pp. 1238–1251, 2020.

[10] M. Romaszewski, P. Głomb, A. Sochan, and M. Cholewa, "A dataset for evaluating blood detection in hyperspectral images," *Forensic science international*, vol. 320, p. 110701, 2021.

[11] M. Al-Sarayreh, M. M. Reis, W. Qi Yan, and R. Klette, "Detection of red-meat adulteration by deep spectral–spatial features in hyperspectral images," *Journal of Imaging*, vol. 4, no. 5, p. 63, 2018.

[12] M. Zulfiqar, M. Ahmad, A. Sohaib, M. Mazzara, and S. Distefano, "Hyperspectral imaging for bloodstain identification," *Sensors*, vol. 21, no. 9, p. 3045, 2021.

[13] A. Taylor, R. van Oorschot, and A. Durdle, "Detection of fresh blood by luminol and dna after walking over various substrates," *Australian Journal of Forensic Sciences*, pp. 1–10, 2023.

[14] F. Zapata Arráez, M. d. l. Á. Fernández de la Ossa, C. García Ruiz, *et al.*, "Emerging spectrometric techniques for the forensic analysis of body fluids," 2015.

[15] A. C. Fonseca, J. F. Pereira, R. S. Honorato, R. Bro, and M. F. Pimentel, "Hierarchical classification models and handheld nir spectrometer to human blood stains identification on different floor tiles," *Spectrochimica Acta Part A: Molecular and Biomolecular Spectroscopy*, vol. 267, p. 120533, 2022.

[16] E. Mistek, L. Halámková, and I. K. Lednev, "Phenotype profiling for forensic purposes: Nondestructive potentially on scene attenuated total reflection fourier transform-infrared (atr ft-ir) spectroscopy of bloodstains," *Forensic Chemistry*, vol. 16, p. 100176, 2019.

[17] A. J. Hart, G. C. Barnes, F. Fuller, A. M. Cornwell, J. Gyula, and N. P. Marsh, "Finding blood in the dark: A comparison of infrared imaging devices for the detection of bloodstains on dark fabrics based on their resolution," *Forensic Science International*, vol. 330, p. 111124, 2022.

[18] S. Cadd, B. Li, P. Beveridge, W. T. O'Hare, and M. Islam, "Age determination of blood-stained fingerprints using visible wavelength reflectance hyperspectral imaging," *Journal of Imaging*, vol. 4, no. 12, p. 141, 2018.

[19] F. Ullah, I. Ullah, R. U. Khan, S. Khan, K. Khan, and G. Pau, "Conventional to deep ensemble methods for hyperspectral image classification: A comprehensive survey," *IEEE Journal of Selected Topics in Applied Earth Observations and Remote Sensing*, 2024.

[20] A. Kaul and S. Raina, "Support vector machine versus convolutional neural network for hyperspectral image classification: A systematic review," *Concurrency and Computation: Practice and Experience*, vol. 34, no. 15, p. e6945, 2022.